Con Edison's New Plasma Tool (PT) for Trenching and Shallow Excavations

Charles Merguerian[1], Silvia Khurrum[2], J. Mickey Merguerian[3], Frank A. Magnotti[4]

[1]Duke Geological Laboratory, 55 Spongia Road, Stone Ridge, NY 12484; CharlesM@Dukelabs.com
[2]Con Edison Research and Development, 4 Irving Place, NYC, NY, 10003; KHURRUMS@coned.com
[3]Dukelabs DSC, 16 Middle Lane, Westbury, NY 11590; Mick@dukelabs.com
[4]Petram Technologies, Inc., 15 Wilkinson Ave., Jersey City, NJ, 07305;
f.a.magnotti@petramtechnologies.com

ABSTRACT

Subsurface trenching for infrastructure beneath the cover of roadways in urban and suburban environments can carry significant production loss due to hidden rock obstructions. Two forms of rock obstructions impede urban trenching and shallow excavations in NYC – 1) rock boulders resting in glacial drift and exposed or 2) shallow buried bedrock ledge. When such subsurface geological differing site conditions occur (unknown boulders or rock ledge), it becomes necessary to use specialized equipment to mitigate the obstructions. Any mitigation technique must fall under strict vibration, dust and noise controls with monitored limits and duration thresholds. Con Edison's Research and Development department together with Petram Technologies Inc. and Duke Geological Laboratory have developed and evaluated a working prototype of a portable, remotely operated electro-hydrofracturing rock-breaking Plasma Tool (PT) to be used in the field for splitting boulders and bedrock ledge. The PT system charges a portable capacitor bank to a high-energy (16-106 kJ = 4-29 watt hr), then delivers that energy through a high-power pulse signal into a probe which has been inserted into a pre-drilled hole filled with electrolytic fluid. High temperature and the acceleration of pressure created inside the rock mass produced from the plasma pressure shock waves results in tensional fracturing within a roughly 1 cubic yard volume within milliseconds with little vibration, noise or dust. Fly rock was mitigated with minimal blanketing - thus the PT is ideal for urban-suburban field use.

Mid-2020 to early 2022 PT field testing and analysis indicated that because NYC's metamorphic bedrock is highly anisotropic with known weakness directions in the form of mineral alignments (foliation, gneissic layering) and internal fractures (joints and faults), the trenching was affected by the relative positioning of excavation drive direction and the internal rock fabrics. Our initial field testing has indicated that driving trench perpendicular to the dominant foliation or metamorphic fabric was much more efficient that driving across or parallel to fabric. Similar to the traditional use of a jack hammer, drill and split, roadheader and other mechanical techniques, breakage into an open face is much more productive than partial or closed-face scenarios. The project research team is working to develop the most efficient depth, length, and energy discharge parameters for the PT probe for Spring 2022 testing.

After over a year of successful testing and development field trials have indicated that production rates are greater, costs are less and construction concerns were mitigated when compared to conventional rock removal methods. We view PT tool as an innovative portable and remotely operated solution in surface to shallow subsurface excavation of boulders and rock ledge obstructions. The lack of noise, vibration, dust and fly-rock as well as highly competitive costs, can make Con Edison's PT use beneficial in urban construction environments.

INTRODUCTION

The excavation of trenches in NYC to install new infrastructure includes areas where rock needs to be removed. Traditional rock breaking techniques utilize drills to make holes from which explosives are inserted for blasting or the rock is chipped/split with pneumatic tools. The use of explosives is not a technique that can be employed in a public street setting and the traditional rock chipping and splitting fracturing process is a slow, labor intensive and noisy.

The project plan is undertaken in two phases. In Phase I a prototype system consisting of a probe, cable and portable trailer with capacitor banks was tested in Alabama on various NYC geological rock samples representing Con Edison's service territory. The results of lab testing and software modeling met Con Edison performance specifications and concluded with the recommendation to undertake Phase II field tests. Phase II embraces three field tests on geological and masonry samples consisting of rock boulders, rock ledge and concrete. The knowledge learned from the field tests, such as constrains and variables, will provide input for prototype retrofits and to understand how to tune the energy releases and probe length for the desired fracturing.

Thus far, our combined efforts in research and development of the PT have shown the tool to be effective in fracturing rock both as boulders and as bedrock ledge into smaller excavatable pieces with below threshold noise, vibration, fly rock nor dust. Preliminary tests and calculations indicate that the tool is 5.5 to 6.5 times more cost effective than traditional means and methods for such excavation. As such the tool may prove to be an important member of the excavation community's toolbox in near future. We have successfully accomplished two phases of PT testing thus far – Phase I (2020) Laboratory Testing and Phase II (2021) Preliminary Field Testing and we are currently planning for a continuation of Phase II (2022) Field Testing which will focus on refinements in equipment and field technique to increase production to retrofit the prototype for a pre-commercial system ready for field use.

Because NYC bedrock and glacial boulders are polymict we have chosen test rocks carefully to include all varieties of NYC bedrock and have concentrated on common glacial lithotypes as well as concrete. In 2020 we collected eleven roughly cubic yard samples of typical NYC bedrock types found stored at the Con Edison Astoria Energy Gas Generating Station yard located at 18-01 20th Avenue, Long Island City, NY 11105 as summarized below in Table 1.

In all, eleven test samples were shipped to Petram's Alabama test facility (Figure 1). Not all samples were tested by Petram but destructive tests were performed on five samples as both buried tests (S1, G3, D1) and also as exposed tests (G4, S3). The results of the tests are described below after a brief discussion of how the PT works and how we implemented its use in our preliminary tests. But, before we delve into the details of the tool and the results of our Phase I and Phase II testing, a brief discussion of the geology of the NYC region includes a simplified view of the configuration of the rock floor, the distinctions between soil (regolith) and ledge (bedrock) and the significance of glacial boulders found in the overburden.

Table 1 – List of typical NYC rock samples shipped to Alabama for Phase I testing.

Con Ed-Petram Phase I Test Rocks

Sample #	L x W x D (in)	Volume (in^3)	Approx. Max. Weight (#)	Formation Name
D1	27 x 20 x 20	10800	1,156	Diabase boulder
D2 (3)	50 x 42 x 33	69300	7,417	Diabase
G1	55 x 27 x 20-24	32670	3,243	Ravenswood Gneiss
G2	47 x 27 x 20	25380	2,519	Fordham Gneiss
G3	42.5 x 35 x 33	49088	4,872	Ravenswood Gneiss
G4	26 x 20 x 20	10400	1,032	Fordham Gneiss
G5A (1)	53 x 42 x 32	71232	7,456	Mafic Gneiss
G5B (2)	46.5 x 35 x 31.5	51266	5,366	Mafic Gneiss
S1	36 x 26 x 11	10296	1,003	Walloomsac Schist
S2	58 x 26 x 15	22620	2,204	Manhattan Schist
S3	36 x 24 x 14	12096	1,179	Hartland Schist
		Max Total Weight (Lbs.) ===>	**37,448**	

Conversions: 1 in^3 = 16.387 cm^3
454 grams (g) = 1 pound (#)
***Note:** Queens Tunnel mafic gneiss ranges 2.9 to 3.3 g/cm^3

Rock Type	Density Range (g/cm^3)	Average Density (g/cm^3)
Mica Schist	2.50-2.90	2.70
Gneiss	2.60-2.90	2.75
Mafic Gneiss	2.80-3.00*	2.90
Diabase	2.80-3.11	2.97

Figure 1 – View of flatbed truck loaded with palleted, plastic-wrapped rock samples as listed above on Table 1.

GEOLOGICAL BACKGROUND

Knowledge of the geological underpinning of subterranean construction offers insights for pre-bid estimates, risk evaluation and as-built cost analysis. Although geologically complex, NYC can be dissected into regions of known rock and soil composition and mechanical properties. In NYC, the construction needs of Con Edison include tunnels, caverns and shafts as well as shallower excavations and trenching for foundations, underpinning and utility lines including those for natural gas, electricity and other forms of cabling. Proper equipment selection for each scope of work is imperative to every construction project and governed by behavior of the materials excavated. Incorrect selections carry heavy cost repercussions in an industry that already possesses razor thin margins.

Although complex, as a result of over a billion years of geological development, NYC can be subdivided into two major layers – 1) **Bedrock** or rock ledge (Layer I) that forms the earth's lithosphere and an overlying sediment blanket that varies from 0' to over 1,000' thick referred to as 2) **Regolith** or soil (Layer II) which is further subdivided into three sub-layers. These layers contain different materials of known properties. Which regolith layers exist? Are there boulders? and How deep and where is the rock? These are basic questions that need answering before a shovel hits the ground.

While nearly impossible to compress over a billion years of history into a few paragraphs the following focuses on geological aspects that have bearing on boulder and rock ledge tool selection for typical shallow-level (0'-100' excavation depth) projects. The key geological control parameters governing means and methods of deep NYC constructs (>100') such as tunnels, shafts and subsurface storage caverns is amply covered in Merguerian (2005a, b; 2008a, b); Merguerian and Ozdemir (2003); Yagiz, Merguerian and Kim (2010) and Vellone and Merguerian (2013).

Geologists reconstruct the history of the Earth by mapping, collecting, and analyzing the rocks, minerals, fossils, and geologic structures preserved in different geologic provinces. What is remarkable about this region is that, within a 100-kilometer (sixty-mile) radius of NYC occur eight major physiographic provinces displaying geologic history from the Proterozoic Era upwards in time (Figure 2).

The most ancient history of this region is imprinted in the complexly deformed metamorphic Proterozoic and Paleozoic crystalline rocks of the **Manhattan Prong** (purple colored area of Figure 2), the crystalline core element of the deeply eroded former mountain chain which now extends northward from central Staten Island through Manhattan, western Queens and the Bronx on into Westchester County and the New England Appalachians. The rocks plunge southward from NYC where they are covered by younger strata only to re-emerge near Philadelphia, PA and southwestward as a core element of the southern Appalachians. Thus, the Manhattan Prong (Layer I) forms a continuous geological substrate, a deeply eroded rock floor beneath all of NYC.

Figure 2 - Physiographic diagram showing the eight major geological provinces in southern New York, northern New Jersey and adjoining states of PA, CT and MA. (From Bennington and Merguerian, 2007.)

BEDROCK LAYER (LAYER I) VS. REGOLITH (LAYER II)

Two major types of geological layers are likely to be encountered in the shallower type of excavations explored in this paper – regolith ("soil") and at some sites bedrock (or "rock ledge") and their removal requires different means and methods. Bedrock or rock ledge is the continuous substrate of crystalline rocks that underlies this region (Layer I). When encountered as rock ledge in an excavation the rock type, structure, orientation and any planes of weakness can vary greatly and study by field operators with some geological training is beneficial. For excavating bedrock ledge of Layer I, tool selection and -use is most effective when selection is based on internal properties of the bedrock (mineralogy, texture and internal structure) as this information will result in more robust utilization.

Boulders can occur sporadically in the glacial regolith of Layer II causing excavation delays. Thus, for Layer II, the geological details that control efficient excavation includes regolith type, thickness and the presence of any rock (as boulders or buried rock ledge). Layers I and II are described separately below.

Layer I - The Bedrock Floor of NYC. Exposed bedrock in NYC and elsewhere around the world is an extension of the earth's lithosphere, has very different mechanical properties than regolith and must be approached differently when excavation needs arise. Details about the different NYC rock types and the geological structure of NYC can be found in Baskerville (1992, 1994), Merguerian (1983, 1994, 1995, 1996) and Merguerian and Merguerian (2004, 2016). For now, let's continue to discuss the "bedrock" as a single layer keeping in mind that it actually hosts a complexly deformed suite of mechanically variable medium- to high-grade metamorphic rocks. Here, the top of rock is a roughly planar surface that eroded over time during the uplift stage (last 250 Ma) of the Appalachian revolution. Before the late Cretaceous Period, uplift of the embryonic Appalachians and deep erosion of the ancient bedrock series over hundreds of millions of years produced a planar top-of-rock surface - the Fall Zone planation surface of Sharp (1929a, b).

As population increased in response to incorporation of the five boroughs into the City of New York in 1898, geologists working for engineering- and construction firms building NYC and environs began to understand the rock floor of the city and publication of bedrock contour maps and geological profiles helped portray the "top of rock" for construction purposes. Based on older maps, well-drilling and existing excavations, Berkey (1910, 1948) and Berkey and Fluhr (1948) published engineering profiles of the rock floor of NYC which showed an essentially flat top of rock surface extending across midtown Manhattan (Figure 3). Solid rock (brown in Figure 3) was typically found close to the surface – typically non-weathered, hard and covered by less than 50' of regolith (orange layer in Figure 3). The shallow overburden has allowed for bedrock to support the vertical load of tall skyscrapers and all elements of the subsurface infrastructure.

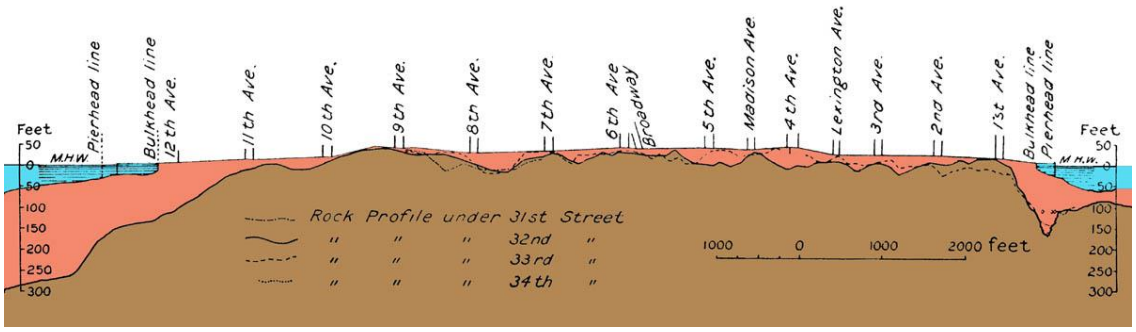

Figure 3 – Profile sections parallel to 31st, 32nd, 33rd and 34th streets in Manhattan showing the thin veneer of regolith (reddish) above the crystalline bedrock (brown). (Adapted and colorized from Berkey 1910, Figure 4.)

The geological profiles E-F, G-H, I-J, L-M, and N-O of Figure 4 from Kemp (1887) shows Manhattan bedrock (olive green [schist+gneiss] and yellow [marble]) is at or near the surface. Northern Manhattan displays highly contorted bedrock at the surface in natural exposures that form prominent ridges over 265' in elevation. By contrast to midtown where rock is close to the surface (See Figure 3.), downtown exhibits thick areas of glacial drift in often deeply incised buried valleys (Moss and Merguerian 2006, 2008). In orange color on the map glacial drift occurs within the 125th Street Manhattanville valley and in the south part of Manhattan as shown in the geological profiles A-B and C-D of Figure 4.

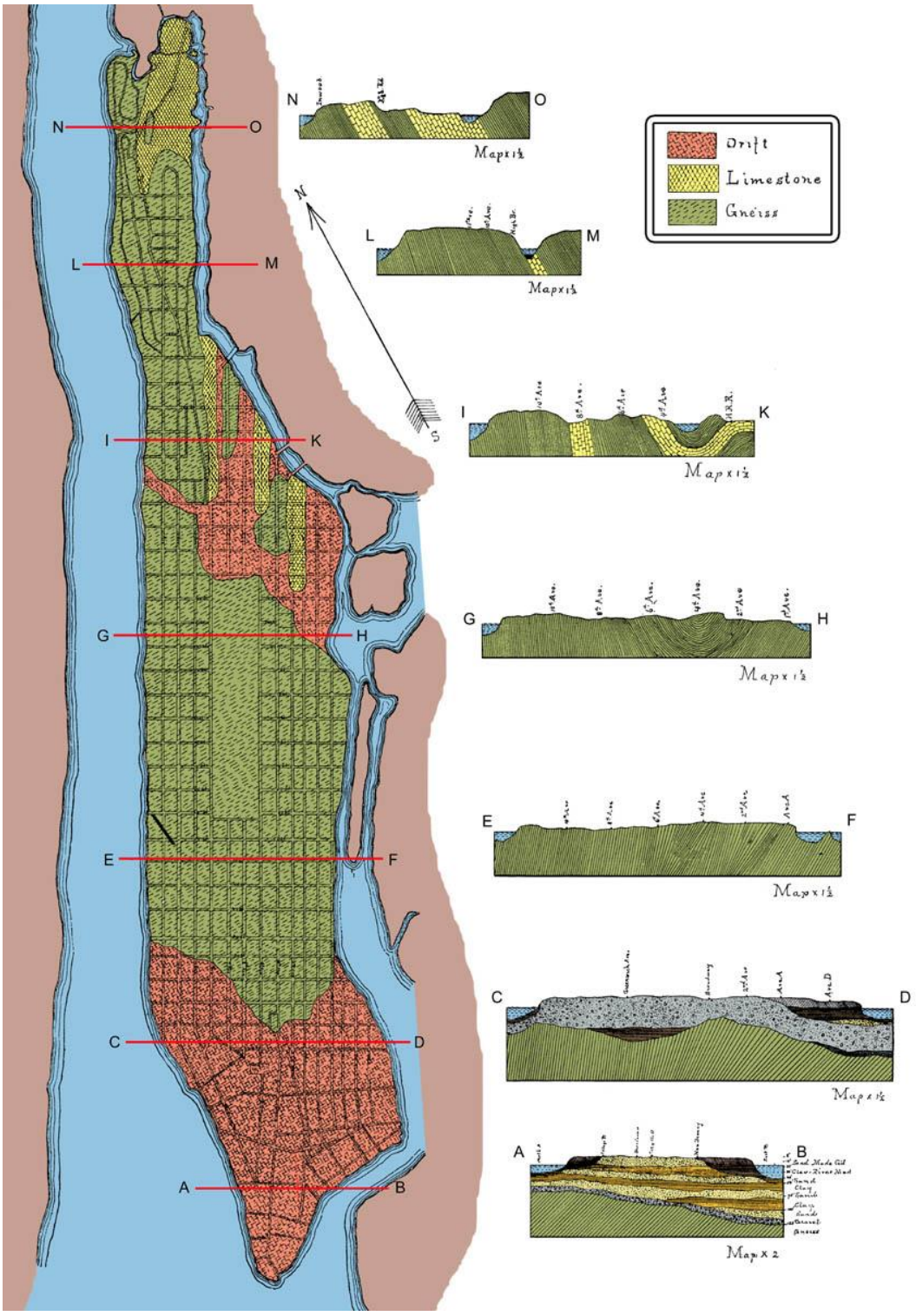

Figure 4 – Geological map of Manhattan and NW-SE serial profiles showing the variable structure of complexly folded NYC bedrock. North of midtown, rock is at or near the surface. Use of the term Limestone [sic] is in key is incorrect – the rock type plotted in yellow is marble, or metamorphosed limestone of the Inwood Formation. Structure section E-F is just north of the profile in Figure 3. (Adapted and colorized from Kemp 1887).

Berkey (1933a, b) provides a detailed profile section of SE Manhattan Island where the glacial drift varies in thickness to over 100’ in places (Figure 5). Note the localized areas of deeply decayed rock (blue) and the variability and structure of bedrock units in the subsurface.

Figure 5 – NW-SE profile section in southeastern Manhattan Island showing steeply inclined Proterozoic and Paleozoic bedrock units and an overlying blanket of Pleistocene glacial drift that averages over 100’ in thickness. Note also the deeply weathered bedrock (blue) at the top of rock. Line of section in red. (Adapted and colorized from Berkey, 1933a, b).

Although bedrock is exposed in Manhattan, the Bronx, westernmost Queens and parts of Staten Island the bedrock slopes below the surface toward the SE and is fully buried beneath most of Queens with very limited bedrock exposed in Long Island City, all of Brooklyn and all of Long Island. A. C. Veatch, in Fuller (1914) provided a structure contour map from borings and well data which documents that this formerly horizontal erosion surface is now tilted southeastward. The regularly spaced, parallel depth-contour lines of Veatch’s map reveals a uniformly sloping bedrock surface tilted ~80’/mile toward the SE.

Many water wells deep enough to reach the basement rocks were drilled mid-century after Fuller's work (deLaguna 1948; deLaguna and Brashears 1948; Suter, deLaguna and Perlmutter, 1949). These mid-century depth to bedrock maps (Figure 6) extend and refines coverage of Veatch’s bedrock map, once again depicting a SE-ward dip of the bedrock surface from where it exists exposed at the surface (brown area to NW corner of map view) to include the ever-thickening blanket of regolith toward the SE in southern Brooklyn (~700’ thick) and southeastern Queens (~1,000’ thick).

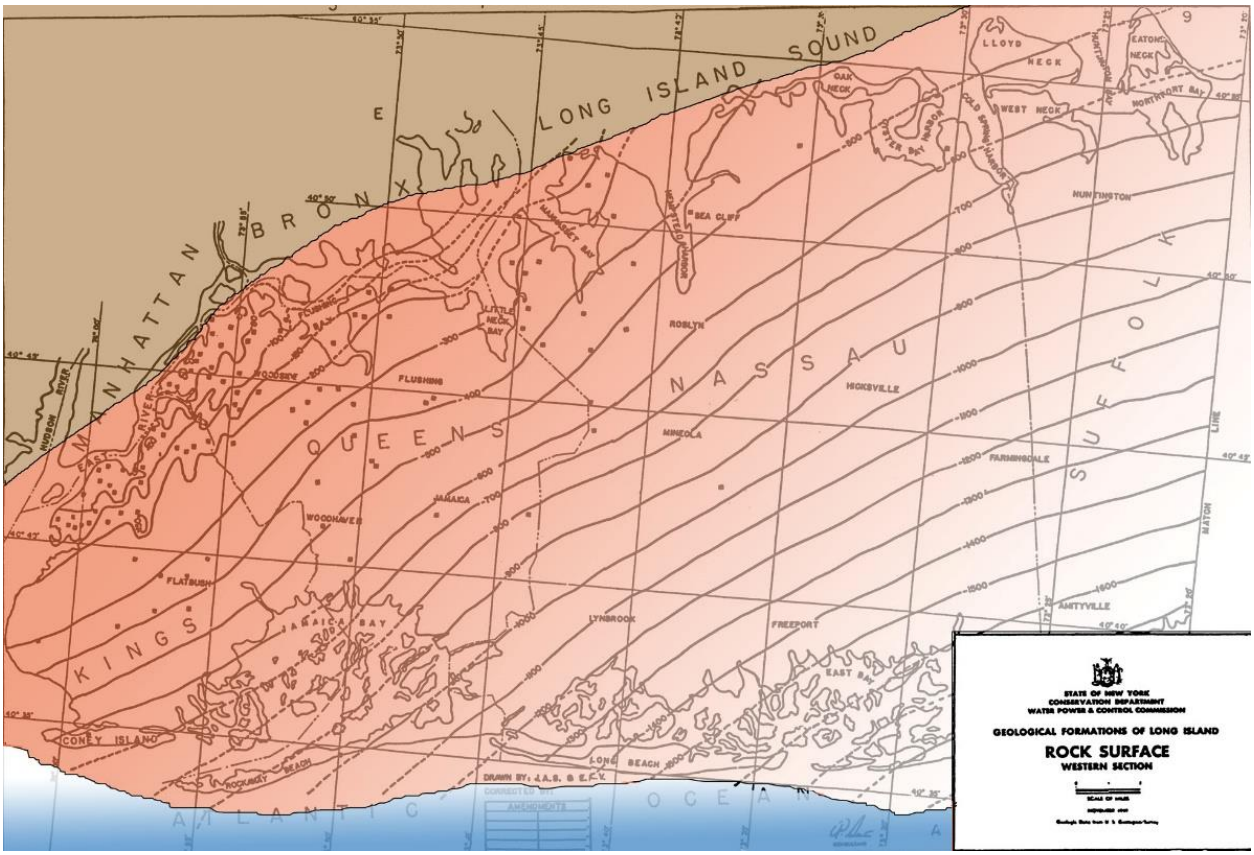

Figure 6 – Rock surface map showing the subsurface depth to bedrock beneath New York City and environs. Areas of exposed bedrock are brown - rock buried by regolith shaded orange. Note the consistent slope of the bedrock surface based on parallel, equal spacing of depth contours. (Adapted and colorized from Suter et al., 1949.)

Layer II – The Soil or Regolith. Where unpaved or built upon, the surface of NYC exposes a blanket of unconsolidated materials collectively designated as regolith - something one can dig with a shovel as contrasted to using a hammer or other mechanical means to break lithified bedrock. Most engineers apply the term "soil" as a synonym of the geologists' term regolith. Regolith can be in-situ residual deposits formed by extensive chemical alteration of underlying bedrock or transported younger regolith layers. In NYC, as a result of multiple glaciations, most regolith has been transported and it may or may not have been derived from underlying local bedrock. Hereabouts, most of the regolith rests on a fresh bedrock surface that has been smoothed, rounded, polished, and scored by features that give indications of Pleistocene glacial flow paths.

To summarize, Layer II in NYC consists of three sub-layers that together constitute the regolith. From the base (oldest) upwards, these include interlayered Cretaceous sediment layers of the Atlantic Coastal Plain which extends from New Jersey through NYC into the subsurface of Long Island (olive colored area in Figure 2). The Cretaceous stratum have been locally

removed by the advance of glacial ice sheets which has left an extensive blanket of Pleistocene glacial and younger Holocene sediment strata. Thus, these NYC sublayers include:

Layer IIA	**Holocene *(Recent)*** beach-, lake-, and river deposits +/- artificial fill.
Layer IIB	**Pleistocene** glacial drift (lake-, till- and outwash- deposits)
Layer IIC	**Cretaceous** clay, silt, sand and gravel layers

GLACIAL BOULDERS – A COMPONENT OF LAYER IIB

Glacial boulders have been dragged at the base of multiple advancing ice sheets from the NW and NE for many miles and show the effects of faceting, polish and rounding as a function of rock type and distance travelled. The resistant NYC bedrock units (gneiss, schist, amphibolite, quartzite and granitoids) are candidates for glacial boulders as are resistant rock types exposed in New Jersey (diabase, some sandstones) and rocks from Westchester County and Connecticut (similar to NYC types with some notable exceptions). Glacial boulders consisting of less resistant schist, marble and serpentinite are rare but have been locally encountered. In fact, careful tracing of boulders of distinctive rock types back to their original limited outcrop-exposure sources in the "upland" areas is what allowed for a multiple glacial flow path hypothesis for NYC (Sanders and Merguerian 1994, 1998; Sanders, Merguerian and Mills 1993). Boulders and bouldery layers typically occur at the base of the glacial regolith and geographically near to where rock unit crops out above sea level but not always! Indeed, glacial dropstones (those melted out and liberated from calved floating ice blocks) can be found at any stratigraphic horizon of Layer IIB and vary in size from pebbles to boulders. Thus, the prediction of glacial boulders is difficult and mitigation techniques need to be in place during the planning stage of projects planned to be built through such glacial strata.

Suffice to say, that encountering boulders in shallow excavations and the need for their timely and thus, cost-effective removal is one of the reasons for specialized equipment such as the EHF PT probe developed by Petram Technologies for Con Edison. Other existing techniques based on site conditions include traditional blasting, expansion grout, hydraulic drill and split techniques, hoe rams and road headers. Boulders are typically rounded and by natural selection are some of the hardest and most resistant, "tough" rock types found in any region. Our experience in NYC excavations indicates that all local rock types have been found. The "tough", volumetrically significant rock types include quartzite, granitoids, migmatite, mafic gneiss, amphibolite and migmatitic mica gneiss,. As such, in areas underlain by glacial strata in western Long Island, Brooklyn and the Bronx, the presence of unknown boulders always poses a construction risk. This can be mitigated with a thorough drilling program or better still, seismic reflection profiling or ground penetrating radar analysis but again these are not foolproof. Boulders must always be expected in sites underlain by glacial strata, especially in the basal till layers.

HOW ROCKS OF LAYER I AND BOULDERS OF LAYER IIB BREAK

Rocks fail (split) much more readily under tensional stress than compressive stress by a factor of 7-10 times depending upon rock type, rock fabric and other intrinsic geological properties. Fracturing of a rock mass is facilitated by the presence of microfractures, mineral

alignments, the proportion of soft minerals (<5 on Mohs' hardness scale) and crystal boundary geometries (rock fabric). Metamorphic rocks contain crystal shape anisotropies based on the degree of alignment and flattening of recrystallized phases during dynamothermal metamorphism – a process that has affected all NYC bedrock units of Layer I. The following section will discuss the technology, use, and effectiveness of the PT.

THE ELECTRO-HYRAULIC FRACTURING PLASMA TOOL (PT)

Our preliminary tests and simulations related to this project demonstrate that Electro-Hydraulic Fracturing is an effective means of rock breakage for underground utility construction projects. The PT system consists of a number of components including an equipment trailer such as shown in Figure 7 which is larger than needed for production use. The larger size accommodates test equipment and storage needs for our preliminary testing phases. The PT system also consists of a capacitor bank (See Figure 7), connecting cable and probe for energy delivery. The PT probes were designed and constructed in-house by Petram Technologies and come in a variety of probe lengths and probe tip configurations (Figure 8).

Component	Details
1x trailer	18'L x 8.5'W x 6.5'H
4x capacitors	Assembly in parallel, 206 μF each, 22kV; Maxwell/GA Series P/N 32349
1x spark gap	L3 Communications P/N ST-300A
2x HV power supplies	30kV; TDK Lambda P/N 202A-30KV-POS-PFC
1x Long Charge Adapter	TDK Lambda P/N 26922100NT
Coaxial cable	Fabricated in-house, 25 feet
Switch control assembly	Fabricated in-house

Figure 7 - PT system main components (trailer and capacitor bank) developed and used during Phase I and Phase II testing (Petram Technologies, Inc.).

After charging of the capacitor bank to a high-energy (16-106 kJ = 4-29 watt hr), the PT probe needs to fit tightly into a pre-drilled hole in the rock mass set for plasma pulse rock target fracturing. Depending upon probe type and length used (12", 18", 24") the drilled hole should accommodate the entire probe length and leave a small (~1") space at the bottom for holding the charge which consists of water and electrolyte. After insertion, the PT probe is weighed down with lead bricks and then blanketed to control fly rock. Upon pulsing, the capacitor bank delivers the stored energy through a high-power pulse signal into the probe. High temperature and the acceleration of pressure created inside the rock mass produced from the plasma pressure shock waves results in tensional fracturing within a roughly 1 cubic yard volume within milliseconds with little vibration, noise or dust. Fly rock was mitigated with minimal blanketing, vibration and noise were well below detectible levels - thus the PT is deemed ideal for urban-suburban field use.

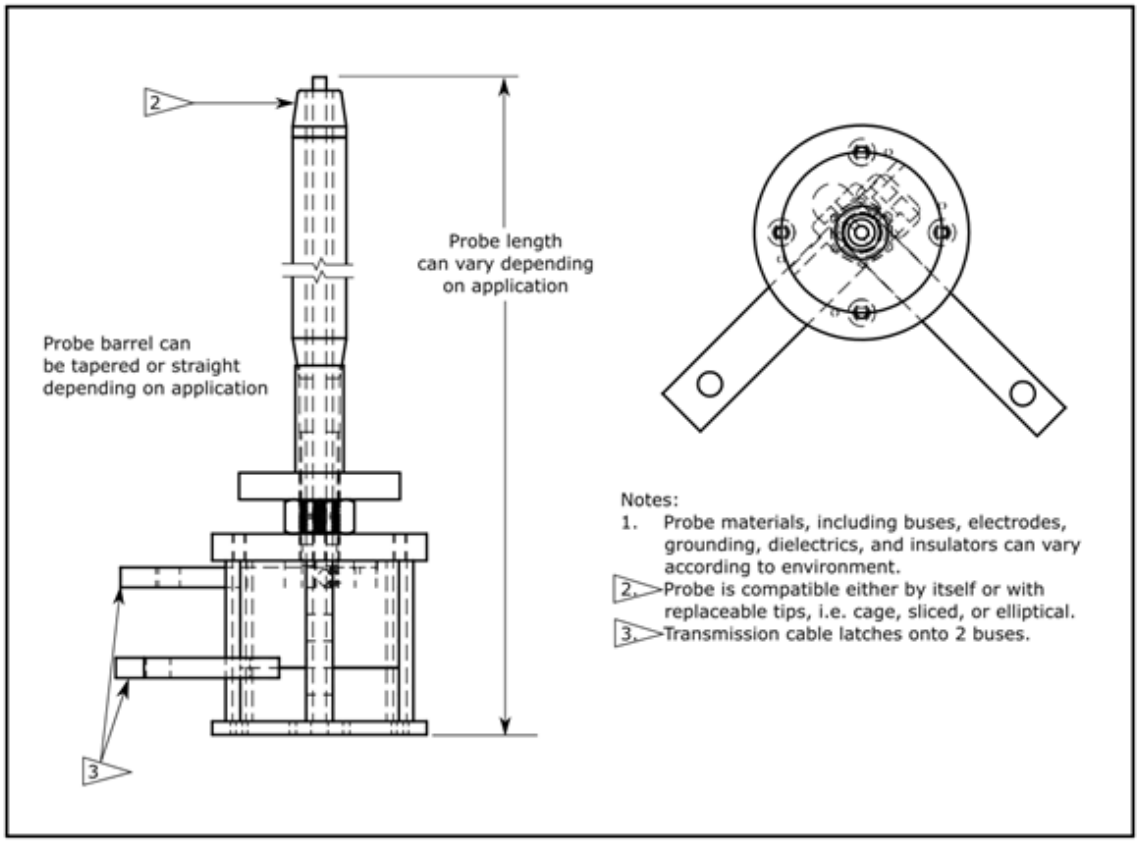

Figure 8 – Image of PT probe and reference drawing. (Petram Technologies, Inc.)

PHASE I VS. PHASE II PT DEVELOPMENT

In 2020, during Phase I development of the Plasma Tool, the Petram team demonstrated that regardless of NYC rock type or construction material (schist, various gneisses, diabase, concrete) that boulders and blocks of rock and material up to a cubic yard in size could be broken apart into smaller pieces (<18") by emitting a plasma pulse from within the center of the mass. Nominally, an 18" deep, 1" wide hole was pre-drilled before the PT probe and water charge were inserted. Phase I tests that were drilled parallel to and perpendicular to gneissic layering in one sample provided similar breakage patterns though we detected a clear difference in breakage style between isotropic igneous rock (diabase) and anisotropic metamorphic rock (gneiss, schist).

For Phase II testing we brought the equipment trailer and test equipment to a Con Edison facility in Rye, NY where NYC gneissic bedrock was exposed in low glaciated exposures. During Phase II we tested for removal of in-situ bedrock ledge in terms of rock fracturing patterns, vibration, dust, fly rock and noise generation and performed a full cost analysis compared to other excavation methods. The summarized results of Phase I and Phase II testing are provided below.

PHASE I

Two types of tests were performed during Phase I – both confined and unconfined. For the confined test large rock samples were held in a wooden test bed crate with the rock sample surrounded and mostly buried by compacted sand (Figure 9). Pipes were installed through the box walls with vibration monitors to simulate and test for PT burst vibration patterns in nearby existing utilities. Below we show a few examples of boxed and unboxed tests.

Of the eleven samples shipped to the Alabama test facility, the following seven samples were tested with the PT (Table 2).

Table 2 – List of seven sample types tested at the Alabama Petram Test facility in 2020.

Petram Test #	Con Ed Sample #	Formation
Buried Test #1	S1	Walloomsac Schist (Foliation parallel to surface)
Buried Test #2	G4	Fordham Gneiss
Buried Test #3	D1	Diabase Boulder
Buried Test #4	Concrete	Aged Concrete 50+ yrs
Buried Test #5	G3	Ravenswood Gneiss
Exposed Test #1	S3	Hartland Schist
Exposed Test #2	G5B (2)	Mafic Gneiss

Originally our specification called for samples that were one (1) cubic yard in size. However, the team had difficulty procuring representative rocks of this exact size. As a result, many samples were larger than originally anticipated. As a result, Petram used this opportunity

to maximize our product/application learning by drilling exactly in the center of each sample to learn the breakage patterns within the samples.

Petram Technologies produced two different types of test rigs:
Five (5) **Buried Test Rigs** to validate against vibration intensity, fragment size, and pipe damage metrics, and,
Two (2) **Exposed Test Rigs** to validate that Petram's tool can be calibrated to the appropriate rock type & size to minimize fly rock.

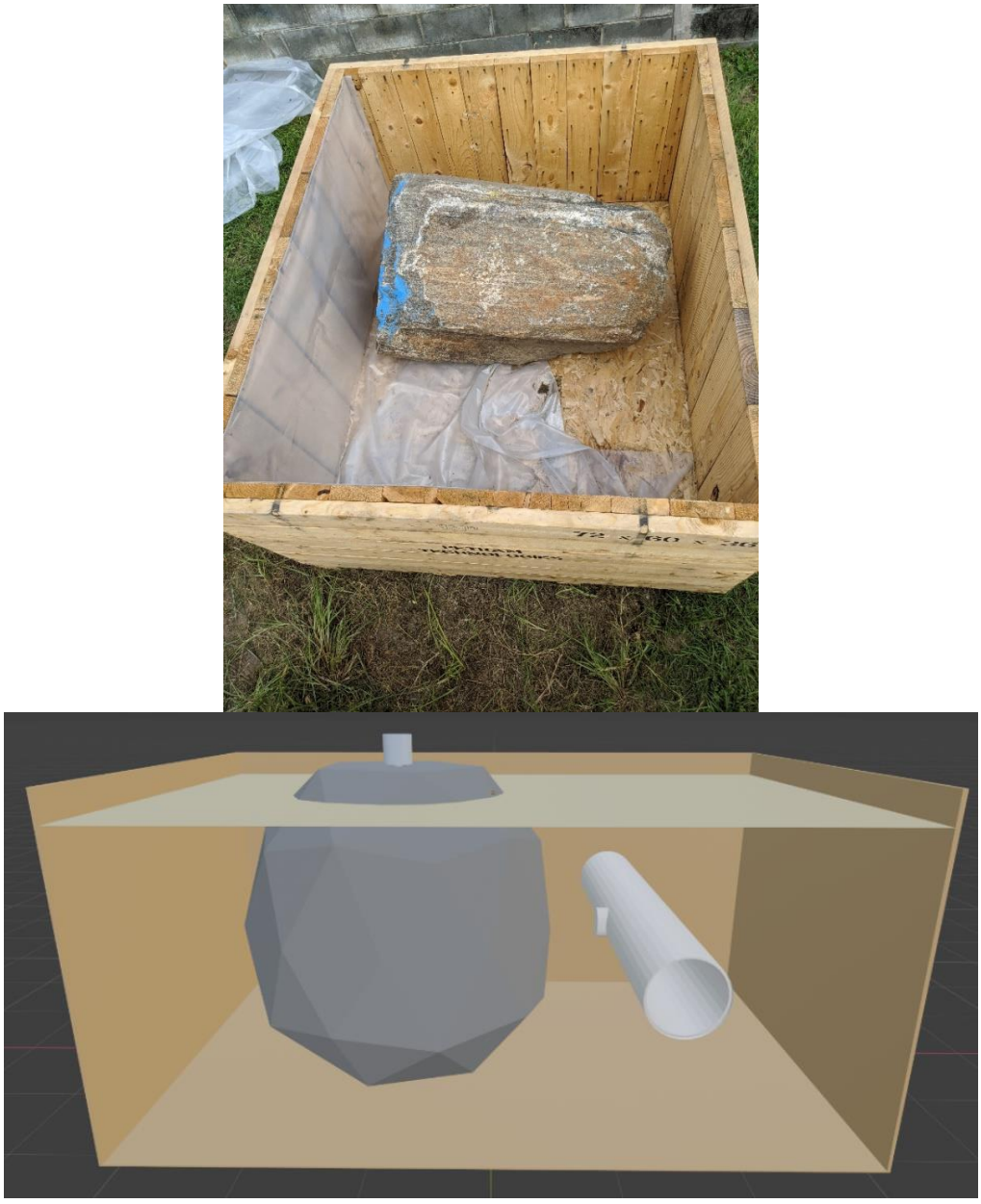

Figure 9 – Image of typical crate being used in a test setup (top) and CAD illustration of test rig setup. The crate external dimensions were 72" long x 60" wide x 36" high and were double-layered with 2" x 6" planks for stability.

The results of four of the seven initial Phase I tests are shown below:

Buried Test #1 (Figures 10A, B)

Con Edison Sample #	S1
Rock Type	Walloomsac Schist
Foliation	Parallel to top surface
Rock Dimensions	25” W x 26” L x 14” H
Test Date	9/5/2020
Probe Length Used	12”
Probe & Hole Diameter	1”
Voltage Used	12kV
Noise Monitor	75 dBA
Dust Monitor	7.6 $\mu g/m^3$
Largest Remaining Fragment	One 27” x 14” x 9”

Before

Figure 10A - Sample S1 before PT test.

After

Figure 10B - Sample S1 after pulsing and unburying.

Results

- After one pulse, the sample cracked along its foliations and broke into the requisite fragment sizes (<16”).
- No flyrock was projected.
- A vibration peak was detected in the pipe, which then reduced to 0 inches/second after 10 milliseconds.
- While peaks were identifiable in the data, the constricted, unnatural environment of the test bed convoluted precise data collection during pulse firing.
- Sound was well below predetermined OSHA requirements.
- No silica dust projection was detected.

Buried Test #2 (Figures 11A, B)

Con Edison Sample #	G4
Rock Type	Fordham Gneiss
Foliation	N/A - Granoblastic texture
Original Sample Dimensions	34” W x 29” L x 29” H
Test Date	9/7/2020
Probe Length Used	12”
Probe & Hole Diameter	1”
Voltage Used	14kV
Noise Monitor	73.2 dBA
Dust Monitor	8.5 $\mu g/m^3$
Largest Remaining Fragment	One 22” x 17” x 14”

Before

Figure 11A - Sample G4 before test.

After

Figure 11B - Sample G4 after pulse and unburying.

Results

- After one pulse, the sample cracked along its incipient foliation and joints.
- Three rock fragments projected three (3) feet from the test fixture. The largest fragment was 3 inches. The speed of these fragments was slow; so it could be managed either via lower voltage setting or a blast blanket.
- A vibration peak was detected in the pipe, which then reduced to 0 inches/second after 25 milliseconds. While peaks were identifiable in the data, the constricted, unnatural environment of the test bed convoluted precise data collection during pulse firing. See
- Sound was well below predetermined OSHA requirements.
- No silica dust projection was detected.

Buried Test #3 (Figures 12A, B)

Con Edison Sample #	D1
Rock Type	Diabase
Foliation	N/A
Original Sample Dimensions	34” W x 27” L x 27” H
Test Date	9/24/2020
Probe Length Used	12”
Probe & Hole Diameter	1”
Voltage Used	9kV
Noise Monitor	74.5 dBA
Dust Monitor	10.3 $\mu g/m^3$
Largest Remaining Fragment	One 24” x 10” x 9”

Before

Figure 12A - Sample D1 before test.

After

Figure 12B - Sample D1 after pulling apart by hand (no tools).

Results

- After one pulse, the sample cracked into 5 clean fragments. Due to the non-metamorphic isotropic crystallinity of diabase, an igneous rock, there were no preferential foliations.
- No rock fragments were projected from the sample.
- A vibration peak was detected in the pipe, which then reduced to 0 inches/second after 15 milliseconds.
- Sound was well below predetermined OSHA requirements.
- No silica dust projection was detected.

Buried Test #5 (Figures 13A, B)

Con Edison Sample #	G3
Rock Type	Ravenswood Granodiorite Gneiss
Foliation	N/A
Original Sample Dimensions	49” W x 32” L x 32” H
Test Date	10/4/2020
Probe Length Used	12”
Probe & Hole Diameter	1”
Voltage Used	14kV
Noise Monitor	85.1 dBA
Dust Monitor	9.2 $\mu g/m^3$
Largest Remaining Fragment	One 20” x 17” x 14”

Before

Figure 13A - Sample G3 before test.

After

Figure 13B - Sample G3 after pulling apart by hand (no tools).

Results

- After one pulse, the gneiss sample kept its form under the sand. Once unburied, the fragments were easily broken apart by hand into multiple fragments.
- No rock fragments were projected from the sample.
- A vibration peak was detected in the pipe, which then reduced to 0 inches/second after 15 milliseconds.
- Sound was well below predetermined OSHA requirements.
- No silica dust projection was detected.

PT technique use benefits that were demonstrated during Phase I testing and simulation were:

1. Each sample was broken into pieces significantly faster than current alternatives such as jackhammering could accomplish.
    a. For reference, Con Edison took 4 hours and broke a drill and saw to break off the piece of mafic gneiss for this experiment. Petram was able to break the rock apart in 15 minutes of total operation time.
2. Each sample was broken into multiple pieces, the majority of which could be removed from a trench with an excavator bucket.
3. Post-pulse, all buried samples were separable by hand. There was also low overall rock displacement and low velocity of the few fragments that did come from the samples.
4. Simulation data indicates that nearby utilities will not be damaged by a pulse traveling through a rock and into 6 inches of sand.
5. Vibration analysis indicated that there were virtually no vibrations 50 milliseconds (on average) after the pulse occurred.
6. The air quality sensor detected virtually no airborne particulate or silica during any test.
7. On average, the maximum sound level from any test is 16x quieter than jackhammers. These sound levels are also 25 milliseconds in duration, in comparison to alternative methods.
8. In light of the COVID-19 epidemic, all results in this report were performed with a one-man operation executing all actions. The information from this phase (Phase I) of the project has unlocked better design considerations and better test results for Phase II.

PHASE II

In 2021 we tested in-situ bedrock and confirmed the findings from the Phase I tests. The Phase II testing allowed us to test the same metrics in an actual field condition to direct product development within Phase II. The Phase II Process Flowchart for executing the test program is shown below (Figure 14).

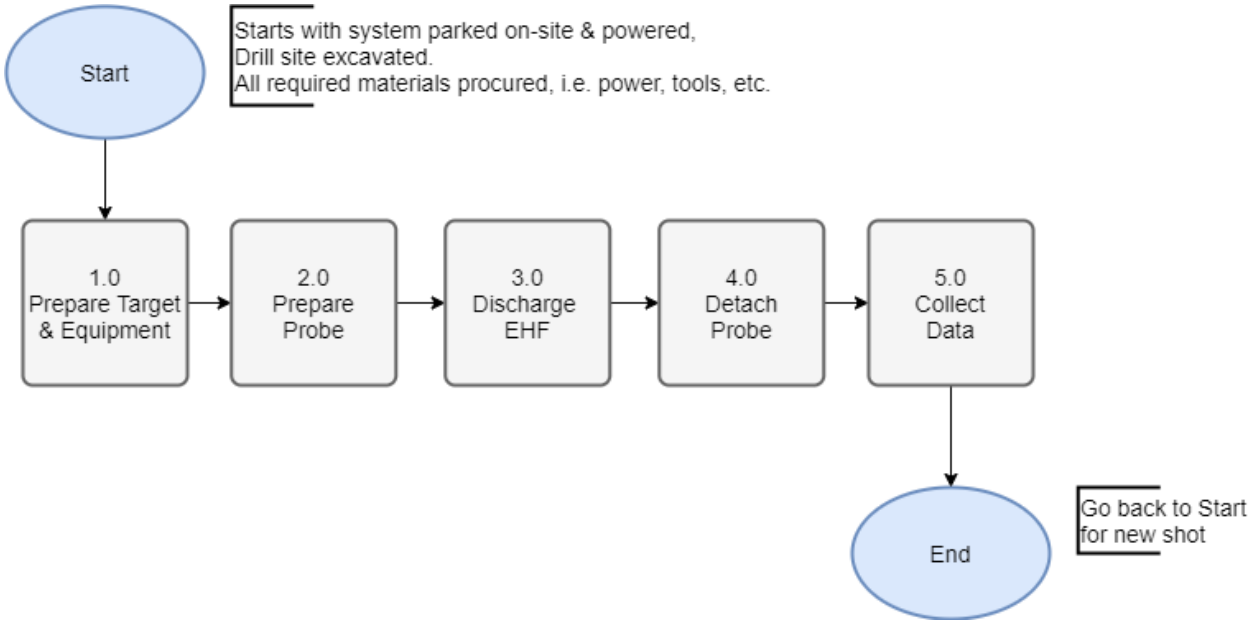

Figure 14 - Process flowchart for Phase II tests.

A Con Edison site in Rye, NY (Figure 15) was examined by Dukelabs and Dukelabs DSC, Inc. together with the Con Edison Research and Development and Petram Technologies on 23 July 2021 where four exposures were evaluated for usefulness in Phase II testing (Figure 16).

Figure 15 - Aerial view of Rye site location (178 Theodore Fremd Avenue, Rye, NY 10580). North to the top. Google Earth Pro image (2021). Outline of Figure 16 shown in white brackets.

Two field visits in late October and early November 2021 were conducted to identify, measure and fully prepare the outcrops for Con Edison's EHF plasma tool on-site implementation and testing. During Phase I of this investigation, Petram had demonstrated consistent success in shattering unconfined boulders, blocks of rock and concrete but the PT was untested in-situ within actual confined NYC bedrock ledge. With guidance from Con Ed construction, we sought out fully open face and partially open face rock mass scenarios.

The Con Edison facility in Rye on Theodore Fremd Avenue (48° 58' 41.66" N Lat. x 73° 41' 34.69" W Long.) offered four areas of naturally exposed bedrock exposures for PPT testing (Figure 16). One of these (Site #3) was selected because the exposure offered an open face exposure, a partially open face exposure and a solitary glacially rounded boulder and was easily accessible from paved lots. Thus, Site #3 was subdivided into Site #3A (open face exposure) and Site #3B (partially open face exposure), and Site #3C (loose boulder). Both 3A and 3B consist of the same rock type, the Hartland Formation. The rocks were representative of typical NYC bedrock, well layered and well foliated and cut by a family of steep to subhorizontal joints.

GEOLOGICAL UNDERPINNING AND CONTROLS

This part of Westchester County is underlain by the Cambrian to Ordovician [roughly 500 million years old (Ma)] Hartland Formation which here consist of steeply inclined, highly deformed and metamorphosed well-layered gneiss, granofels, schist and minor amphibolite – the

products of former deep-seated dynamothermal metamorphism during protracted Paleozoic compressional tectonics (mountain building). The rocks contain varying proportions of feldspars, quartz, micas (muscovite and biotite), garnet and kyanite with lesser amphibole and minor opaque minerals.

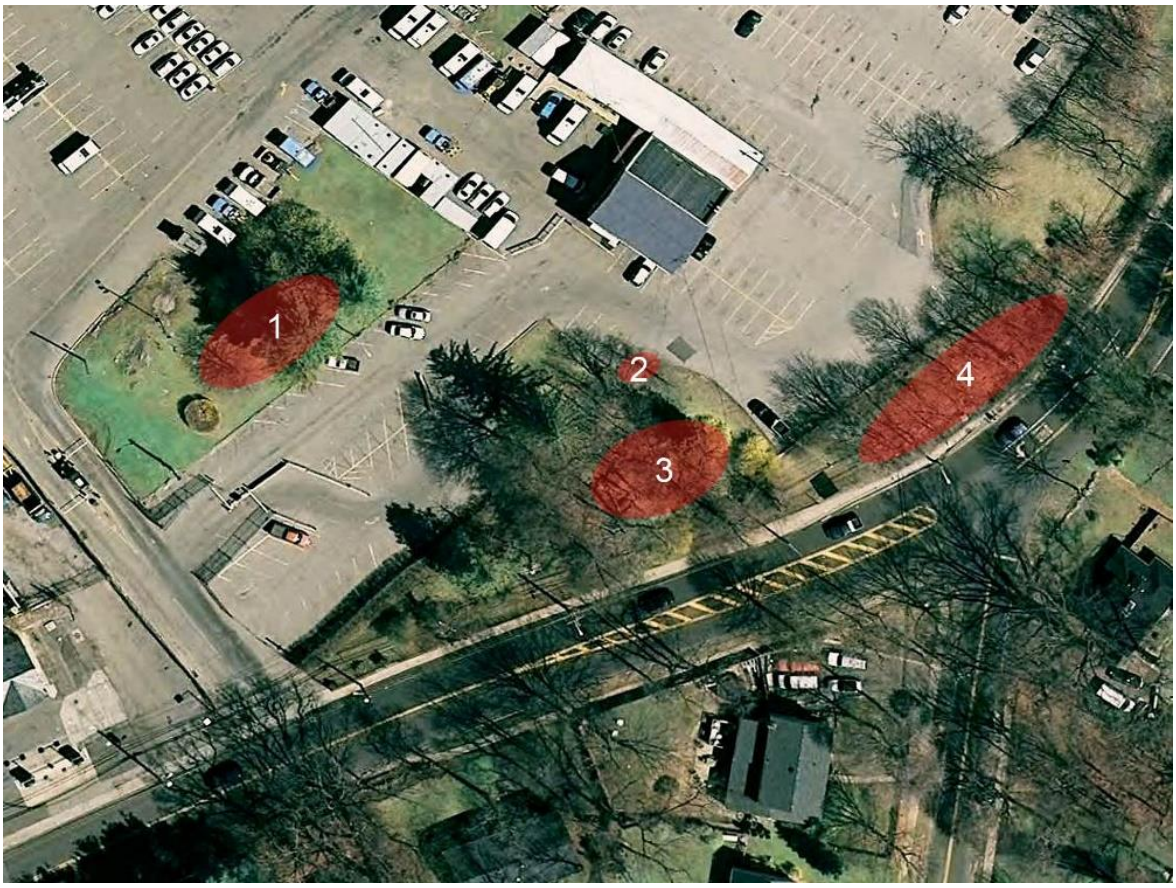

Figure 16 – View of four main outcrop areas consisting of NE-trending migmatitic gneiss, granofels, schist and minor amphibolite of the Hartland Formation, a common constituent of NYC bedrock. Site #3 was selected for reasons of equipment accessibility and support and ability to plan for three modes of plasma tool field use to best simulate actual trench construction in solid, confined rock ledge. Site #3 is also desirable for the lack of post-excavation visual disturbance as the area is tree-bound and well-vegetated. (Google Earth Pro image, 2021.)

Metamorphism resulted in a major transformation of former interbedded sands, shales and volcaniclastic materials into the foliated rock types now exposed at the Rye yard including gneiss, granofels, schist and minor amphibolite (Figure 17). Although compositionally similar, the rock types transition into one another and are stitched together by cm to 10s of cm thick injections of foliated granitoid that overall produces a migmatite rock mass (mixed igneous and metamorphic rock). The granitic veins show evidence of metamorphism and flattening into the plane of foliation. These types of rocks, found in subvertical orientation and glacially eroded as here, represent the worst-case scenario for trenching and associated rock excavation – thus ideal for our Phase II tests.

Figure 17 – View of Hartland Formation consisting of migmatitic interlayered gneiss, granofels, schist and foliated lit-per-lit granitoids (light-colored injections) up to 15 cm in thickness. The geological structure is dominated by NE-trending compositional layering S_0 and parallel penetrative S_1 foliation oriented ~N35°E, 87°SE. Pen scale is 15 cm in length. (Dukelabs image taken 17Nov21.)

S_1 Penetrative Foliation. Foliation in metamorphic rocks is the result of recrystallization under compressive stress which results in parallel mineral growth of platy and linear minerals (mostly micas and amphiboles) and crystal-shape flattening of non-platy feldspars and quartz which together predominate in the Hartland rock mass. Together, the platy and linear minerals and other flattened phases stitch together to produce the primary metamorphic fabric (termed S_1). Measurements and mapping of the steeply inclined foliation (S_1) is provided in the Dukelabs Pre-Burst data sheets for each of the two test sites (3A, 3B). Suffice to say that the S_1 foliation or metamorphic fabric trends parallel to the typical Appalachian trend in the NYC region, roughly N35°E and here dips very steeply at roughly 85°SE. This imparts an intrinsic fabric or weakness (splitting) direction throughout the rock mass which is facilitated by the parallel J_1 joint set which was exploited in all of the successful PT tests.

J_1, J_2, J_3 AND J_4 Joints. Joints are natural dislocations within any rock mass, typically produced after the main phases of deformation. They are similar to faults in that they are fractures but show no relative offset. The outcrops are well-foliated, well-layered and cut by four families of NE- and NW-trending steep joints (J_1, J_2, and J_3) and random gently inclined sheeting joints (J_4). J_1 joints were the most prominent. These are foliation joints parallel to the inherent metamorphic fabric and parallel compositional layering (S_0) of the Hartland Formation which offer planes of weakness. The J_1 joint set was quite obvious in the 3A test site but less obvious in the more massive 3B site but still offers a favorable splitting surface for use of the PT, as expanded upon below.

The J_1 set is fully controlled by aligned minerals defining the S_1 metamorphic fabric and parallel S_0 compositional layering. They vary from open weathered joints a few cm wide filled with soil and roots to mm-scale and tight planar and healed joints. The J_2 joints are steeply dipping, typically planar, spaced, tight and healed and sometimes with weathered surfaces. They cut the subvertical foliation and J_1 joints at a nearly orthogonal high angle. Thus, the exposures demonstrated an inherent blocky weakness in two directions (J_1 x J_2) which resulted in nearly rectangular breakage patterns in the meter to cm scale. The S_1, J_1 and J_2 structural elements are cut by a random set of conjugate, planar J_3 joints which are possibly related to the J_2 joints. These are sporadic but different from J_2 in that they are moderately dipping, typically non-continuous and planar to curved in nature. The J_4 joint set are very gently inclined and related to vertical lithostatic load reduction resulting from profound uplift and erosion that post-dates the former 450 Ma development of the metamorphic rocks deep within the Earth.

Indeed, the phase relationships of the included metamorphic minerals indicate that the rock mass acquired its S_1 metamorphic fabric at depths of 20-30 km. Since we see these rocks at the Earth's surface today clearly over the 500 Ma time span since development that much uplift and erosion has occurred to expose them. The vast change in lithostatic load produces subhorizontal joints (J_4) the result of lithospheric unloading. The J_4 set is typically weathered, open (mm^s to cm^s) and commonly filled with soil and root material. Testing showed that the NE-trending, steeply inclined S_0 compositional layering, parallel S_1 foliation and J_1 joints were primary failure surfaces during PT testing. Orthogonal J_2 joints were failure surfaces as well but the J_3 and J_4 joints were also important in rock failure patterns.

Glaciation. The Hartland Formation occurs here in a roche moutonée structure that shows strong glacial polish and glacial striae indicative of glacial ice flow from both the NE to SW (overall shape of exposure) and NW to SE directions (local glacial scratches and grooves). The most recent glaciers in NYC flowed from NE to SW (Sanders and Merguerian 1993) and have sculpted and modified the bedrock in this region.

The exposure at site #3 is roughly 400 ft^2 in extent and shows a gently sloping up-glacier NE side and a jagged SW edge created by down-glacial "plucking" or erosion of that side of the rock exposure (Figure 18). After raking off the thin soil and root covering on 03 November 2021, the overall asymmetrical shape of the bedrock knoll was revealed and we identified a drill location and open face.

Figure 18 – Southward view of the Site #3A bedrock knoll showing the overall roche moutonée structure, the marked drill site for PT pulse #1 and the open face that we wanted to break against with the PT. The outcrop displays a gently inclined, glacially polished NE facing slope (foreground) and a steep, jagged S-facing rough edge in the background where the overriding glacial ice sheet plucked the rock mass along internal weaknesses (typically joints) as it passed over. (Dukelabs image view toward the S taken 03Nov21.)

PT EXPERIMENTAL TEST PLAN

Most of the time, bedrock excavations in NYC will show similar "typical" steeply inclined NE-trending fabrics and as such site #3 offers a prime example of bedrock expectation in NYC and deemed a perfect setting for our planned PT application and experimentation. Clear and comfortable weather conditions prevailed both days and allowed for careful data recording which included geological data, PT machine performance data, vibration, noise and air quality measurements and removed rock volume data. Baseline noise, vibration and airborne dust were measured a day earlier by Tectonic Engineering. With representatives from Petram Technologies Inc., Con Edison Inc., Duke Geological Laboratories and Dukelabs DSC, Inc. present (~20 in attendance), three of the seven tests occurred on 17 November with the first two at Site #3A and the third one at Site #3B. The next day, four tests using different drill hole approaches directed toward further experimental excavation of Site #3B. As the geological

backdrop for the Rye test site has been amply covered above, this paper will now chronicle the tests from a purely geological perspective. Overall, seven tests were conducted on 17-18 November 2021 – we share a few of these below.

Annotated PT Phase II Test Results – 17+18 November 2021

Site #3A – Pulse #1 (17Nov21; PT Burst @ 11:22 AM)
10:48 AM Target Prep; Total Rock Removed: 0.75 yards^3

Pulse #1 was successful in breaking loose a large block of Hartland gneiss (45.5" x 26" x 23") and four smaller blocks from the exposure into a soil-filled cleft below the open face (Tables 3 and 4). The smaller blocks measured 29" x 13" x 9", 26" x 10" x 7", 16" x 16" x 5" and 8" x 6" x 5" and many fractures were detected in the in-situ bedrock after workers rotated the larger block outward from the exposure to expose the bottom. The bottom of the block showed the effects of the pulse, where the deeper rock was pulverized nearer to the probe tip.

The larger block was moved up and out from the outcrop during the pulse (Figures 19A, 19B). It failed along the geological weaknesses measured in the pre-pulse investigation – the S_1 foliation and parallel J_1 joint set, the J_2 joint set and a subhorizontal weathered J_4 sheeting joint. The pulse weakened the surrounding rock, setting the stage for a significant volume of breakage during Pulse #2 after redrilling at the same site.

Figure 19A - View of dislodged 0.58 yard^3 block of Hartland gneiss that moved up and out from exposure the result of pulse #1. Failure took place along surrounding joints which were weathered, filled with soil and roots and seem to have absorbed and localized pulse energy. The shape of the block is controlled by the geological surfaces S_1, J_1, J_2, J_3 and J_4 as shown below in the annotated view of the same block. The block was moved easily with a backhoe and later broken into smaller pieces by the backhoe bucket. (Dukelabs image taken 17Nov21.)

Figure 19B – Same view as above Figure 19A showing the outline of preferential breakage planes S_1, J_1, J_2 and J_3 that surround and cut through the large block that was displaced by pulse #1. The block was bounded along the bottom and top by sub-horizontal J_4 sheeting joints. (Dukelabs image taken 17Nov21.)

Although Figures 19A and 19B suggest that the tool was ineffective in breaking the large 0.58 yard^3 block, after it was mechanically removed from the exposure by the backhoe it broke readily into smaller pieces along internal joints upon pounding with the backhoe bucket. This would lead one to believe that the PT pulse weakened the large block internally and although it was "lifted" out of the exposure by the pulse along weathered joints surrounding it, internal damage was indeed significant. Overall, we calculated 0.75 yards^3 of material excavated with pulse #1 in a very short period of work time.

Site #3A – Pulse #2 (17Nov21; PT Burst @ 12:19 PM)
12:00 PM Target Prep; Total Rock Removed: 1.8 yards^3

A new probe hole was drilled by workers for pulse #2 across from the main J_1 failure joint shown in Figure 20. Based on the breakage patterns observed the new hole was placed 12" from the new open face that was left by removal of the large block loosened in pulse #1. The second and final pulse at Site #3A was very effective in breaking the rock mass into many smaller pieces (Figure 21). We measured 5 blocks that failed along S_1, J_1, J_2, J_3 and J_4 joint surfaces and took a sample. These were 90" x 42" x 18", 26" x 17" x 10", 26" x 14" x 11", 25" x 17" x 8" and 10" x 9" x 3" and ~25 brick-sized chunks of bedrock that were easily broken and moved by the pry bar and backhoe work team (Figure 22). We suspect that pulse #1 was more effective than obvious since fracturing in the lower section of the exposure became noticeable after the second pulse. Pulse #2 removed roughly 1.8 yards^3 of rock (Figure 23). Together, the two pulses (#1 + #2) resulted in roughly 2.55 yards^3 of rock removed from site #3A (Table 4).

Figure 20 – View of drilled hole before placing PT probe into rock mass for second test pulse. Hole is 12" inches from newly exposed active open face which was revealed after rotating the large block from pulse #1 away from the outcrop. The newly open face is controlled by the S_1 and J_1 weakness surfaces. The effectiveness of the initial pulse can be seen by comparing this view with previous images of the #3A site (Figure 18). (Dukelabs image taken 17Nov21.)

Figure 21 – Post pulse #2 view of bedrock showing internal fracturing and failure along the J_1, J_2 and J_4 joints. Rocks were readily peeled from exposure by mechanical means and methods. (Dukelabs image taken 17Nov21.)

Figure 22 – Workers prying loose bedrock pieces easily with pry bars after pulse #2. After removal from the pulse zone, the broken pieces (Figure 23) together accounted for roughly 1.8 cubic yards of rock removed after the second pulse. (Dukelabs image taken 17Nov21.)

Figure 23 – Largest piece of bedrock (to left of bucket) was peeled from top of exposure after pulse #2. It failed along a steep J_2 joint and a low-angle, weathered J_4 sheeting joint. All of the blocks were readily removed with pry bars and the backhoe. Note the angular, blocky shape of bedrock blocks – failure controlled by main geological weaknesses in rock mass. Rocks removed by the initial pulse were moved by backhoe, beyond this view, to the left of the image. (Dukelabs image taken 17Nov21.)

Site #3B – Pulse #3 (17Nov21; PT Burst @ 3:02 PM)
2:34 PM Target Prep; Total Rock Removed: 0 yards^3

The location was switched to Site #3B for the third and final pulse of the day with limited effectiveness. This was a difficult rock removal scenario by any means and methods as only a partially open face was exposed and the 24" probe was drilled below the active open face (Figure 24). The probe hole was drilled by the drill crew and gently widened to accept the probe.

Figure 24 – View of partially open face of outcrop at Site #3B showing the location of the probe hole to be drilled by crew. (Dukelabs image taken 17Nov21.)

The pulse removed almost no rock and the probe was ejected upwards during PT use, the probable result of a slightly oversized 1-3/8" drill – subsequent holes (Pulses 5 through 7) were drilled with a smaller, 1" bit. Yet, radial fracturing around the drill hole was detected immediately after the pulse (Figure 25) and the next day, after some relaxation, the fractures extended preferentially parallel to the S_1xJ_1 (~N35°E) orientation. The J_2 joint face (~N56°W, 75°SW) was undisturbed and no rock was removed from the outcrop. Visible on the partial open J_2 joint face, some low-angle J_4 joints opened overnight to produce incipient fractures (Figure 26) that allowed for manual excavation of the fractured rock mass – though results were inferior to Site #3A production. Test measurements for Days 1 and 2 can be seen on Tables 3 and 4.

As in any closed- or partially open face scenario with no open space to break into, results were limited for Site #3B pulses (4 through 7) as shown in Table 4. Yet, the outcrop was affected as visible fracturing was detected at the base of the exposure and workers were able to remove many brick-sized blocks from the exposure after a few pulses (See Figures 25, 26). Phase III of our investigations will focus on tool utilization techniques for tough rock removal scenarios such as shown at Site #3B where two of the five pulses failed for various reasons.

Figure 25 – View of radial fractures subtended around pulsed drill hole after pulse #3 at site #3B. Note how the incipient fractures (drawn blue lines) preferentially parallel the S_1 foliation and parallel J_1 joints, both trending about N35°E. Center line of compass points (upward) toward true North. Overnight relaxation of rock mass had taken place. (Dukelabs image taken 18Nov21.).

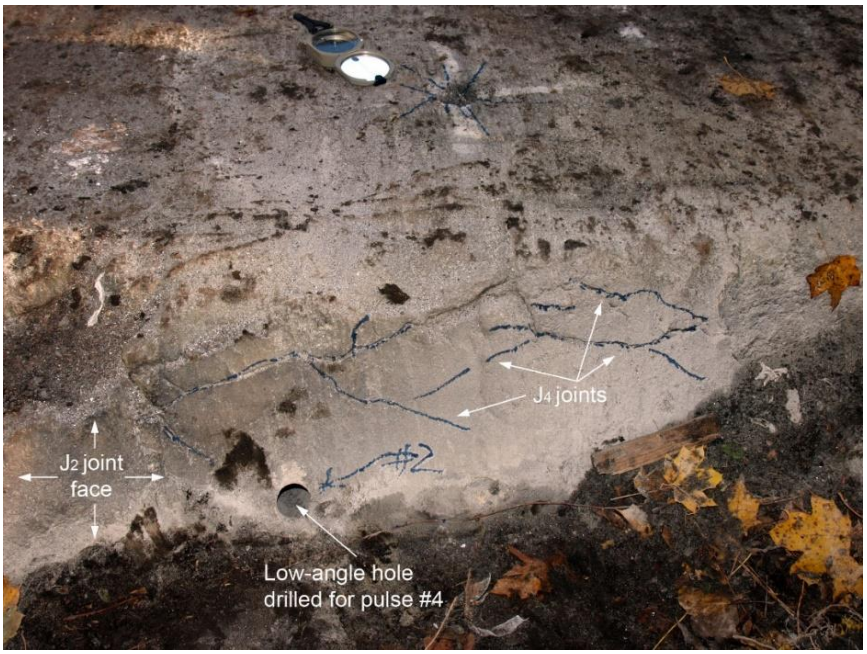

Figure 26 – Low-angle view of undisturbed J_2 joint face (~N56°W, 75°SW) and incipient opening of J_4 sheeting joints after overnight relaxation of rock mass. Compass points towards true North. Note location of 25° low-angle hole drilled for pulse #4. (Dukelabs image taken 18Nov21.)

Tables 3 and 4 – PT pulse and production data.

Table 3 - Pulse Data - 178 Theodore Fremd Avenue, Rye NY

Pulse #	Date	Target Prep Time	Pulse Time	Pulse Time Interval (min.)	Site Location	Drill Type	Hole Depth	Drilled Diameter	Distance to Open Face	Probe Depth	Probe Type	kV Used	Result
1	17-Nov-21	10:48 AM	11:22 AM	34	3A	Toku	25.75"	1-3/8"	14.5"	24"	24" Stinger	16	Internally fratured block loosened along J1, J2, J3 and J4 joints
2	17-Nov-21	12:00 PM	12:19 PM	19	3A	Toku	25.75"	1-3/8"	12"	24"	24" Stinger	16	Very effective pulse resulting in significant rock mass fracturing
3	17-Nov-21	2:34 PM	3:02 PM	28	3B	Toku	26.5"	1-3/8"	17.75"	24"	24" Stinger	16	Radiating short fractures around drill hole preferentially parallel to J1
4	18-Nov-21	9:19 AM	10:19 AM	60	3B	Toku	26.5"	1-3/8"	0"	24"	24" Stinger	16	No rock removed but incipient fracturing noted
5	18-Nov-21	11:50 AM	12:11 PM	21	3B	Toku	10"	1"	6.5"	10"	24" Stinger	16	Small amount of rock removed; fly rock detected
6	18-Nov-21	1:20 PM	1:50 PM	30	3B	Toku	25.75"	1"	18"	24"	24" Stinger	16	Almost no visible damage; some increase in incipient cracks
7	18-Nov-21	2:21 PM	2:32 PM	11	3B	Toku	25.75"	1"	18"	12"	24" Stinger	16	Almost no visible damage; some increase in incipient cracks

Table 4 - Pulsed Rock Removed - 178 Theodore Fremd Avenue, Rye NY

Pulse #	Date	Site Location	Number Rock Pieces	Size Range	Average Size	Cubic Yards Removed (Calc.)
1	17-Nov-21	3A	5	5" - 45.5"	~20"	0.75
2	17-Nov-21	3A	~30	3"-90"	~30"	1.8
3	17-Nov-21	3A	0	-	-	0
4	18-Nov-21	3B	20	2"-5"	3"	0.1
5	18-Nov-21	3B	26	1"-8"	3.5"	0.07
6	18-Nov-21	3B	10	3"-6"	4.5"	0.07
7	18-Nov-21	3B	0	-	-	0

DUKE

PRODUCTION ANALYSIS

Preliminary production and cost analysis of the Plasma Tool (PT) shows significant production, cost, and safety benefits when compared to conventional methodologies of in-situ rock removal. The analysis looked at historic production in man hours / cubic yard (MH / CY) of two different conventional methods and compared it to preliminary production rates achieved by the PT on 17 November 2021 (three pulses at sites #3A and #3B). Conventional methods used for comparison were limited to acceptable methods when in proximity of existing utilities (pneumatic drill and removal methods and hydraulic rock splitting methods).

Pneumatic drill and rock removal for the same region of New York has an average production rate of 7.58 MH / CY (n = 61). The hydraulic rock splitting methods has an average production rate of 10.17 MH / CY (n = 33). During our field tests of the PT on 17 November 2021, we achieved an average production rate of 0.86 MH / CY (n = 3). Our initial field test, two out of three of the pulses were successful in fracturing rock that can be easily excavated. The production analysis accounted for this lost time in creation of the 0.86 MH / CY.

A time-cost study was provided by Dukelabs DSC Inc. which collected all time, laborer's unions, equipment used, and all materials used during the test. Labor cost was then derived based on their union's straight time rate and time on site. Separating cost into two categories: 1) **Production Time** - which is the time used on the operation, what most would consider being 'in production' and 2) **Test Time** which is time used by during the Phase II field test to record metrics, collect data, take photographs, and generally use time for things that would not occur in a production-based construction setting. Equipment rates were derived from the blue book rate per piece of equipment and material rates were based on actual invoices.

Once we had the Phase II field test's times separated into Production Time and Testing Time we were able to produce a preliminary production cost based on our limited (n=3) data points. Our preliminary though limited results indicate that the PT was able to average $485 in cost / CY removed which accounted for all labor, equipment, and material costs during the field test (Table 5). This cost is 5.5 to 6.5 times less costly than existing methods.

Table 5 – Production and preliminary cost calculation summary for Phase II field tests

Date	Field Report #	Pulse Location	Pulse #	Lithology Description	Production (Hours / CY)	Total Production ($ / CY)
11/17/21	1	3A	1	Migmatitic Schist/ Gneiss	0.64	$ 361.95
11/17/21	1	3A	2	Migmatitic Schist/ Gneiss	0.35	$ 198.08
11/17/21	1	3B	1	Migmatitic Schist/ Gneiss	∞	∞
Average (Includes Time for Shot 3B - #1 with no Production QTY)					0.86	$ 484.63

SUMMARY AND DISCUSSION

The objective of this Con Edison Research and Development project was to develop and field test a portable technology that employs NASA-funded Petram electro-hydraulic fracturing (EHF) technology, suitable for breaking rock and concrete in an urban infrastructure. It uses an EHF process, where stored electric power is released over a short duration pulse through two electrodes submerged in pre-drilled holes containing water. The energy release generates very high temperatures that transform the water directly to plasma which then creates a high-pressure shock wave that exceeds the tensile strength of the rock mass causing pervasive fracturing. The technology is suitable for both rock and concrete applications.

In dealing with removal of rock ledge or bedrock at any site, we have learned that inherent weaknesses in the rock mass must be fully understood before attempting PT pulses. Similar to traditional mechanical removal techniques, our mid-November 2021 experiments clearly showed that PT drill holes must be placed away from pre-existing fractures, preferably near a live or open-edge of rock masses. Pulse #1 showed that pulse energy is preferentially absorbed in soil-filled, weather joints and fractures so these should be avoided. Here, the deeply weathered soil and root-filled joints (J_1 and J_4) tended to absorb PT energy and reduce the efficacy of the PT burst.

The vast difference in excavation performance between the open face site #3A and partially open face site #3B (Table 4) points to a fundamental difference in approach at the two adjacent sites. At site #3A we successfully broke rock against the S_1 x J_1 structural weakness. In this case the force of the pulse was directed toward the weakness planes offered by the penetrative foliation (S_1) and subparallel foliation joints (J_1). By contrast and with limited production result as shown in Table 4, site #3B testing was attempting to break the bedrock perpendicular to the $S_1 + J_1$ foliation fabric by attempting to rupture the rock mass into a secondary joint face (J_2) or across the foliation. Thus, the directional properties of NYC bedrock proved quite important in dictating test results and will be considered during future Phase II testing and development.

What is more, calibration of electrical charges and probe length and type will accompany our future investigations. The main development focus forward will be in 1) achieving precision in rock breaking for any excavations in tight spaces and 2) achieving production speed and efficiency in removing large volumes of rock during trenching in both length and depth. We view this tool as being effective as an artisanal, controlled rock removal tool – understanding the geological structural weaknesses will help increase the efficacy of the Con Edison plasma tool. These are some areas that will be explored during Phase II tests planned for Spring/Summer 2022.

To determine success our team will be evaluating performance, cost, safety and usability aspects of a complete and fully developed automated solution compared to the traditional rock demolition tools used today. By increasing our PT testing we will then be able to compare these data to our database of production costs for mechanical and hydraulic means and mechanisms to develop a full cost comparison between various toolings. Our preliminary data indicates PT use is 5.5 – 6.5 times less costly than conventional methods.

REFERENCES

Cited reports by the first and third authors can be found at www.Dukelabs.com under the Publications tab.

Baskerville, C. A., 1992, Bedrock and engineering geologic maps of Bronx County and parts of New York and Queens counties, New York: U. S. Geological Survey Miscellaneous Investigations Series Map I-2003 (scale 1:24,000).

Baskerville, C. A., 1994, Bedrock and engineering geology maps of New York County and parts of Kings and Queens counties, New York and parts of Bergen and Hudson counties, New Jersey: U. S. Geological Survey Miscellaneous Investigations Series Map I-2306 (2 sheets; colored maps on scale of 1/24,000).

Bennington, J Bret, and Merguerian, Charles, 2007, Geology of New York and New Jersey: Physical Geology Textbook Supplement, 24 p. *in* Essentials of Geology with Geology of New York and New Jersey: Thomson Brooks/Cole, 510 p.

Berkey, C. P., 1910, Areal and structural geology of southern Manhattan Island: Annals New York Academy of Sciences, v. 19, p. 247-282.

Berkey, C. P., 1933a, Engineering geology of the City of New York: in Berkey, C. P., ed., Guidebook 9, New York Excursions, New York City and vicinity: *in* 16th International Geological Congress, United States, 1933, Washington, D. C., United States Government Printing Office, p. 77-123.

Berkey, C. P., 1933b, New York City and vicinity: International Geological Congress 16th, United States, Guidebook 9, New York excursions, 151 p.

Berkey, C. P., 1948, Engineering geology in and around New York: in Creagh, Agnes, ed., Guidebook of Excursions: Geological Society of America, 61st Annual Meeting, New York City, p. 51-66.

Berkey, C. P.; and Fluhr, T. W., 1948, Engineering geology of New York City water supply, p. 121-135 *in* Creagh, Agnes, ed., Geological Society of America Annual Meeting, 61st, New York City, Guidebook of Excursions, 135 p.

deLaguna, Wallace, 1948, Geologic correlation of logs of wells in Kings County, New York: New York State Department of Conservation, Water, Power and Control Commission Bulletin GW-17, 35 p.

deLaguna, Wallace; and Brashears, M. L., Jr., 1948, The configuration of the rock floor in western Long Island New York: New York State Department of Conservation, Water, Power and Control Commission, Bulletin GW-13, 32 p.

Fuller, M. L., 1914, The geology of Long Island, New York: U. S. Geological Survey, Professional Paper 82, 231 p.

Kemp, J. F., 1887, The geology of Manhattan Island [N. Y.]: New York Academy of Sciences Transactions, v. 7, p. 49-64.

Merguerian, Charles, 1983, The structural geology of Manhattan Island, New York City (NYC), New York (abstract): Geological Society of America Abstracts with Programs, v. 15, no. 3, p. 169 (only).

Merguerian, Charles, 1994, Stratigraphy, structural geology, and ductile- and brittle faults of the New York City area, p. 49-56 *in* Hanson, G. N., *chm*., Geology of Long Island and metropolitan New York, 23 April 1994, State University of New York at Stony Brook, NY, Long Island Geologists Program with Abstracts, 165 p.

Merguerian, Charles, 1995, The Taconic problem - alive and well in New York City (NYC) (abs.): Geological Society of America Abstracts with Programs, v. 27, no. 1, p. 68.

Merguerian, Charles, 1996, Stratigraphy, structural geology, and ductile- and brittle faults of New York City, p. 53-77 *in* Benimoff, A. I. and Ohan A. A., *chm.*, The Geology of New York City and Vicinity, Field guide and Proceedings, New York State Geological Association, 68th Annual Meeting, Staten Island, NY, 178 p.

Merguerian, Charles, 2005a, Geological controls on effective hard-rock TBM tunneling in crystalline terrains, 11 p. *in* 84th Annual Meeting, 9-13 January 2005, Compendium of Papers CD-ROM, Transportation Research Board of the National Academies.

Merguerian, Charles, 2005b, Lithologic and structural constraints on TBM tunneling in New York City (NYC), p. 704-724 *in* Hutton, John D. and Rogstad, W.D., *eds.*, Rapid Excavation and Tunneling Conference, 2005 Proceedings Society of Mining, Metallurgy, and Exploration, 1371 p.

Merguerian, Charles, 2008a, Evaluating geological controls on hard rock excavation, New York City, NY: *in* Proceedings, Manhattan On the Rocks, American Society of Civil Engineers, Metropolitan Section, 08 May 2008, 31 p.

Merguerian, Charles, 2008b, Geological controls on means and methods of hard rock excavation, New York City, NY: p. 79-109 *in* Gorring, M. L., ed., Environmental and Engineering Geology of Northeastern New Jersey, Geological Society of New Jersey, XXV Annual Conference Proceedings, 17 October 2008, 111 p.

Merguerian, Charles, 2014, Field geology of southern New England: Field guide for Hofstra University Field Course, Geology 143E, 15-21 March 2014, 263 p.

Merguerian, Charles; and Merguerian, J. Mickey, 2004, Geology of Central Park – From rocks to ice: *in* Hanson, G. N., *chm*., Eleventh Annual Conference on Geology of Long Island

and Metropolitan New York, 17 April 2004, State University of New York at Stony Brook, NY, Long Island Geologists Program with Abstracts, 24 p.

Merguerian, Charles; and Merguerian, J. Mickey; 2016b, Trip A-5 - Field guide to Isham, Inwood, and Central parks, NYC, NY: p. 163-189 in Alexander A. Gates and J Bret Bennington, *eds.*, New York State Geological Association, 88th Field Conference, 30 September - 02 October 2016; 446 p.

Merguerian, Charles; and Ozdemir, Levent, 2003, Rock Mass Properties and Hard Rock TBM Penetration Rate Investigations, Queens Tunnel Complex, NYC Water Tunnel #3, Stage 2: p. 1019-1036 in Robinson, R.A. and Marquardt, J.M., eds., Rapid Excavation and Tunneling Conference, 2003 Proceedings, 1334 p.

Moss, C. J., and Merguerian, Charles, 2006, Evidence for multiple glacial advances and ice loading from a buried valley in southern Manhattan: *in* Hanson, G. N., *chm*., Thirteenth Annual Conference on Geology of Long Island and Metropolitan New York, 22 April 2006, State University of New York at Stony Brook, NY, Long Island Geologists Program with Abstracts, 16 p.

Moss, C. J., and Merguerian, Charles, 2008, Bedrock control of a boulder-filled valley under the World Trade Center site: *in* Hanson, G. N., *chm*., Fifteenth Annual Conference on Geology of Long Island and Metropolitan New York, 12 April 2008, State University of New York at Stony Brook, NY, Long Island Geologists Program with Abstracts, 13 p.

Sanders, J. E.; and Merguerian, Charles, 1994, Glacial geology of the New York City region: p. 93-200 *in* Benimoff, Alan; and others, eds., Geological Association of New Jersey Annual Meeting, 11th, Somerset, NJ, 14-15 October 1994, Field guide and proceedings, 296 p.

Sanders, John E., and Merguerian, Charles, 1998, Classification of Pleistocene deposits, New York City and vicinity – Fuller (1914) revived and revised: p. 130-143 *in* Hanson, G. N., *chm*., Geology of Long Island and Metropolitan New York, 18 April 1998, State University of New York at Stony Brook, NY, Long Island Geologists Program with Abstracts, 161 p.

Sanders, J. E.; Merguerian, Charles; and Mills, H. C., 1993, "Port Washington deltas" of Woodworth (1901) revisited: pre-Woodfordian Gilbert-type deltas revealed in storm-eroded coastal bluff, Sands Point, New York (abstract): Geological Society of America Abstracts with Programs, v. 25, no. 6, p. A-308 (only).

Sharp, H. S., 1929a, A pre-Newark peneplane and its bearing on the origin of the lower Hudson River: American Journal of Science, v. 218, p. 509-518.

Sharp, H. S., 1929b, The fall zone peneplane: Science, v. 69, p. 544-545.

Suter, Russell; deLaguna, Wallace; and Perlmutter, N. M., 1949, Mapping of geological formations and aquifers of Long Island, New York: New York State, Department of Conservation, Water, Power and Control Commission, Bulletin GW-18, 212 p.

Vellone, D.A., and Merguerian, Charles, 2013, Structural geology and its influence on the kinematics of rock stability: A critical foundation consideration in urban environments: American Society of Civil Engineers, Metropolitan Section, Conference on Foundation Challenges in Urban Environments, 16 May 2013, 15 p.

Yagiz, S., Merguerian, C., and Kim, T., 2010, Geological controls on the breakthrough of tunnel boring machines in hard rock terrains, p. 401-404 *in* Zhao, Labiouse, Dudt, and Mathier *editors*: EUROCK'10, Rock Mechanics in Civil and Environmental Engineering, Proceedings of the ISRM European Rock Mechanics Symposium.